Article

TRANSPARENT PROCESS

THE EMBO JOURNAL

p38γ and p38δ reprogram liver metabolism by modulating neutrophil infiltration

Bárbara González-Terán[1,†], Nuria Matesanz[1,†], Ivana Nikolic[1,†], María Angeles Verdugo[1,2], Vinatha Sreeramkumar[1], Lourdes Hernández-Cosido[3,4], Alfonso Mora[1], Georgiana Crainiciuc[1], María Laura Sáiz[1], Edgar Bernardo[1], Luis Leiva-Vega[1], Elena Rodríguez[1], Victor Bondía[1], Jorge L Torres[5,6], Sonia Perez-Sieira[7,8], Luis Ortega[3,4], Ana Cuenda[2], Francisco Sanchez-Madrid[1], Rubén Nogueiras[7,8], Andrés Hidalgo[1], Miguel Marcos[5,6] & Guadalupe Sabio[1,*]

Abstract

Non-alcoholic fatty liver disease (NAFLD) is a major health problem and the main cause of liver disease in Western countries. Although NAFLD is strongly associated with obesity and insulin resistance, its pathogenesis remains poorly understood. The disease begins with an excessive accumulation of triglycerides in the liver, which stimulates an inflammatory response. Alternative p38 mitogen-activated kinases (p38γ and p38δ) have been shown to contribute to inflammation in different diseases. Here we demonstrate that p38δ is elevated in livers of obese patients with NAFLD and that mice lacking p38γ/δ in myeloid cells are resistant to diet-induced fatty liver, hepatic triglyceride accumulation and glucose intolerance. This protective effect is due to defective migration of p38γ/δ-deficient neutrophils to the damaged liver. We further show that neutrophil infiltration in wild-type mice contributes to steatosis development by means of inflammation and liver metabolic changes. Therefore, p38γ and p38δ in myeloid cells provide a potential target for NAFLD therapy.

Keywords diabetes; inflammation; obesity; steatosis; stress kinases
Subject Categories Immunology; Metabolism; Molecular Biology of Disease
DOI 10.15252/embj.201591857 | Received 20 April 2015 | Revised 18 December 2015 | Accepted 22 December 2015 | Published online 3 February 2016
The EMBO Journal (2016) 35: 536–552

Introduction

Non-alcoholic fatty liver disease (NAFLD) is the leading cause of chronic liver disease in Western countries and estimates of its worldwide prevalence range from 6 to 35% (Vernon *et al*, 2011). NAFLD refers to a wide spectrum of liver damage, ranging from simple steatosis caused by intracellular triglyceride accumulation to inflammation (non-alcoholic steatohepatitis [NASH]), fibrosis, and cirrhosis (Marchesini *et al*, 2003). NAFLD is a main cause of cryptogenic cirrhosis and may also predispose to hepatocarcinoma (Farrell & Larter, 2006).

The pathogenesis of NAFLD is strongly associated with insulin resistance, obesity and type 2 diabetes (Fabbrini *et al*, 2010). However, the mechanisms involved in the accumulation of triglycerides in the liver and subsequent hepatocellular damage are multifactorial and not completely understood. Metabolic deregulation and hepatic steatosis have been linked to stress signaling (Sabio & Davis, 2010; Sabio *et al*, 2010), and the activation of stress kinases in steatosis and obesity suggests a role for these proteins in this disease (Sabio & Davis, 2010). The stress-activated protein kinase group consists of two subfamilies: p38 mitogen-activated kinases (p38 MAPKs) and c-Jun N-terminal kinases (JNKs). While the role of JNKs in the development of steatosis has been widely studied (Sabio *et al*, 2008, 2009), less is known about the role of the p38 MAPK signaling pathway. In mammals, four p38 MAPK isoforms have been identified: p38α, -β, -γ, and -δ. Despite biochemical evidence of specific roles for the individual isoforms, redundancy and embryonic lethality have impeded attempts to establish their distinct functions *in vivo* (Sabio & Davis, 2014). Embryos lacking p38α die due to defects in placental development (Adams *et al*, 2000; Allen *et al*, 2000; Tamura *et al*, 2000), but mice lacking p38β, -γ, and -δ are viable without any obvious defects under basal conditions (Beardmore *et al*, 2005; Sabio *et al*, 2005). Kinases p38γ and -δ were recently shown to control inflammation by regulating

1 Fundación Centro Nacional de Investigaciones Cardiovasculares Carlos III, Madrid, Spain
2 Department of Immunology and Oncology, Centro Nacional de Biotecnología/CSIC, Madrid, Spain
3 Bariatric Surgery Unit, Department of General Surgery, University Hospital of Salamanca, Salamanca, Spain
4 Department of Surgery, University of Salamanca, Salamanca, Spain
5 Department of Internal Medicine, University Hospital of Salamanca-IBSAL, Salamanca, Spain
6 Department of Medicine, University of Salamanca, Salamanca, Spain
7 Department of Physiology, CIMUS, University of Santiago de Compostela-Instituto de Investigación Sanitaria, Santiago de Compostela, Spain
8 CIBER Fisiopatología de la Obesidad y Nutrición (CIBERobn), Santiago de Compostela, Spain
*Corresponding author. Tel: +34 91453 12 00; E-mail: guadalupe.sabio@cnic.es
†These authors contributed equally to this work

macrophage production of tumor necrosis factor (TNF)-α (Risco *et al*, 2012; Gonzalez-Teran *et al*, 2013) and T-cell activation (Criado *et al*, 2014); moreover, p38δ also influences neutrophil inflammatory responses in the lung (Ittner *et al*, 2012).

Since chronic inflammation is central to the progression of NAFLD, we aimed to define the role of p38γ and p38δ in the development of this disorder. We detected elevated liver expression of p38δ in a cohort of obese patients with NAFLD and found that p38γ and p38δ are responsible for the development of steatosis and NASH in three animal models of NAFLD: mice fed a high-fat diet (HFD), mice fed a high-fat fructose diet (HFF), and mice fed a methionine–choline-deficient (MCD) diet. Lack of p38γ and p38δ in myeloid cells impaired neutrophil migration to the liver and thus protected against steatosis and further hepatic damage. These results highlight the importance of p38 kinases and neutrophils in NAFLD and open a new avenue for the treatment of this disease.

Results

p38γ and p38δ are overexpressed in NAFLD

Analysis of liver biopsies from obese NAFLD patients (body mass index [BMI] > 35 kg/m^2) revealed elevated mRNA expression of *MAPK13* (p38delta) compared with non-obese individuals without NAFLD, and a similar tendency was detected for *MAPK12* (p38gamma) (Fig 1A). Further, among individuals with a BMI < 35 kg/m^2, hepatic *MAPK12* and *MAPK13* mRNA was elevated in individuals with liver steatosis compared with control individuals without liver disease (Fig 1B). Western blot analysis confirmed higher liver expression of p38δ protein in obese individuals with steatosis (Fig 1C). To corroborate these results in a mouse model of steatosis, we studied the expression and activation of p38γ and p38δ in livers from mice fed a methionine–choline-deficient (MCD) diet, which induces macrovesicular steatosis and is widely used in NASH research (Anstee & Goldin, 2006). MCD diet increased the mRNA expression of p38δ (Fig 1D) and induced the activation of p38γ and p38δ after 1 week (Fig 1E). This activation remained high during the 3 weeks of the diet (Fig 1E and F). These results indicate a possible role of p38γ and p38δ in the development of steatosis.

Mice lacking p38γ and p38δ are protected against MCD-induced steatosis

To study how these kinases affect the development of fatty liver, we fed a MCD diet to WT mice and mice lacking p38γ (p38γ$^{-/-}$), p38δ (p38δ$^{-/-}$), and both p38γ and p38δ (p38γ/δ$^{-/-}$). Compared with MCD-diet WT mice, MCD-diet p38γ$^{-/-}$ and p38δ$^{-/-}$ mice showed only a slightly milder liver steatosis as evaluated by H&E and Oil Red staining (Appendix Fig S1A); in contrast, the development of steatosis and inflammation was strongly attenuated in p38γ/δ$^{-/-}$ mice (Fig 2A and Appendix Fig S2A). These findings were confirmed by biochemical analysis of hepatic triglyceride content (Fig 2B and Appendix Fig S1B). Moreover, whereas MCD diet increased serum levels of alanine transaminase (ALT) in WT, p38γ$^{-/-}$, and p38δ$^{-/-}$ mice, the level in p38γ/δ$^{-/-}$ mice was significantly lower, indicating milder liver necrosis (Fig 2C and Appendix Fig S1C). The appearance of steatosis protection only in mice doubly deficient for p38γ and p38δ probably reflects the previously described partial functional redundancy between the two isoforms (Risco *et al*, 2012; Gonzalez-Teran *et al*, 2013).

An early event in MCD-induced choline deficiency is the appearance in liver of oxidized lipids, DNA, and proteins. Assay of thiobarbituric acid reactive substances in the livers of MCD-fed animals detected lower oxidized lipid content in p38γ/δ$^{-/-}$ mice than in WT animals, correlating with lower levels of hydrogen peroxide in the double-knockout mice (Fig 2D). Liver fibrosis is a hallmark of NASH. Livers of MCD-diet WT mice expressed higher levels of *Col1a1* and *Acta2* than MCD-diet p38γ/δ$^{-/-}$ mice (Fig 2E), correlating with higher Masson's trichrome staining (Fig 2F). These results demonstrate that p38γ/δ$^{-/-}$ mice are protected against MCD-diet-induced steatosis and NASH.

Inflammation plays a key role in the pathogenesis of NAFLD, and the development of hepatic steatosis is associated with increased liver infiltration by myeloid cells (Tiniakos *et al*, 2010). p38γ/δ kinases regulate inflammation through the control of TNF-α production in macrophages and Kupffer cells (Risco *et al*, 2012; Gonzalez-Teran *et al*, 2013), and p38δ modulates neutrophil motility in lung disease (Ittner *et al*, 2012), prompting us to examine the mRNA expression levels of myeloid cell markers and pro-inflammatory cytokines in mice fed the MCD diet. Liver expression

Figure 1. p38γ and p38δ are up-regulated in NAFDL.

A Left: qRT–PCR analysis of mRNA expression of *MAPK12* (p38gamma) and *MAPK13* (p38delta) in liver extracts prepared from obese patients with alcoholic fatty liver disease (NAFLD) and control individuals without NAFLD. mRNA expression was normalized to the amount of *Gapdh* mRNA (n = 11–74). Right: representative H&E-stained liver sections. Scale bar: 50 μm.

B Left: qRT–PCR analysis of mRNA expression of *MAPK12* (p38gamma) and *MAPK13 (*p38delta) in liver extracts prepared from control patients with NAFLD/non-alcoholic steatohepatitis (NASH) and control individuals without NAFLD/NASH. mRNA expression was normalized to the amount of *Gapdh* mRNA (n = 9–11). Right: representative H&E-stained liver sections. Scale bar: 50 μm.

C Quantification of immunoblot analysis of p38δ expression in liver extracts prepared from obese patients with NAFLD and individuals without NAFLD. Representative blots are shown (n = 7–40).

D qRT–PCR analysis of *Mapk12* (p38gamma) and *Mapk13 (*p38delta) mRNA expression in liver extracts prepared from wild-type mice (WT) fed a diet deficient in methionine and choline (MCD) or control diet (ND) for 3 weeks; mRNA expression was normalized to the amount of *Gapdh* mRNA (n = 5–10).

E Immunoprecipitation analysis of activation and protein levels of p38γ and p38δ isoforms in liver extracts prepared from WT fed a MCD or ND diet for the times indicated.

F Immunoprecipitation analysis of activation and protein levels of p38γ and p38δ isoforms in liver extracts prepared from WT fed a MCD or ND for 3 weeks (n = 5). Western blot against vinculin was used to assay the protein amount in the total lysate (TL) used for each IP. Protein expression was normalized to vinculin.

Data information: Data are means ± SEM. *P < 0.05; **P < 0.01. Statistical significance by two-tailed Student's t-test. Characteristics of patients and controls were compared by means of χ^2 or Mann–Whitney U-tests.

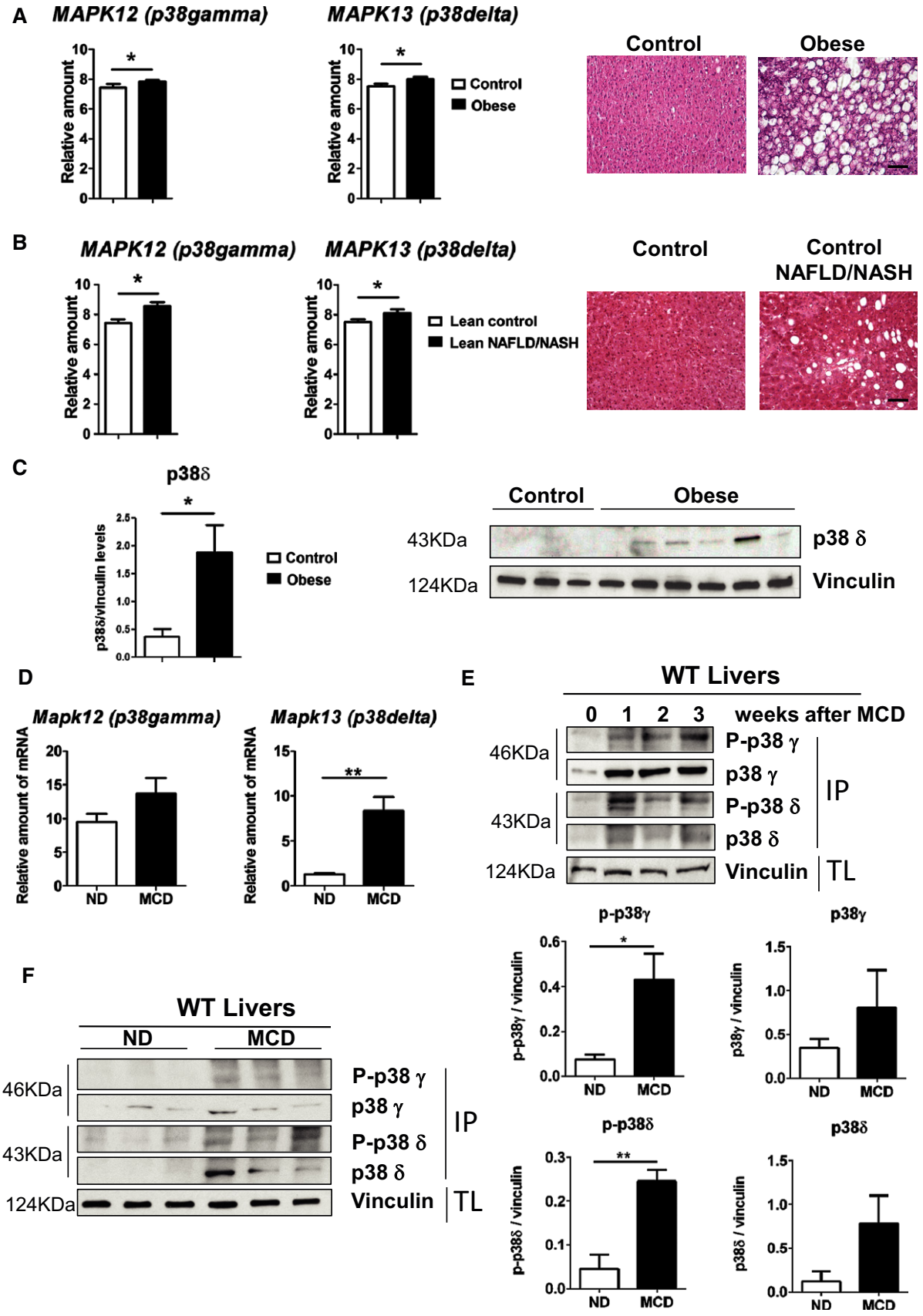

Figure 1.

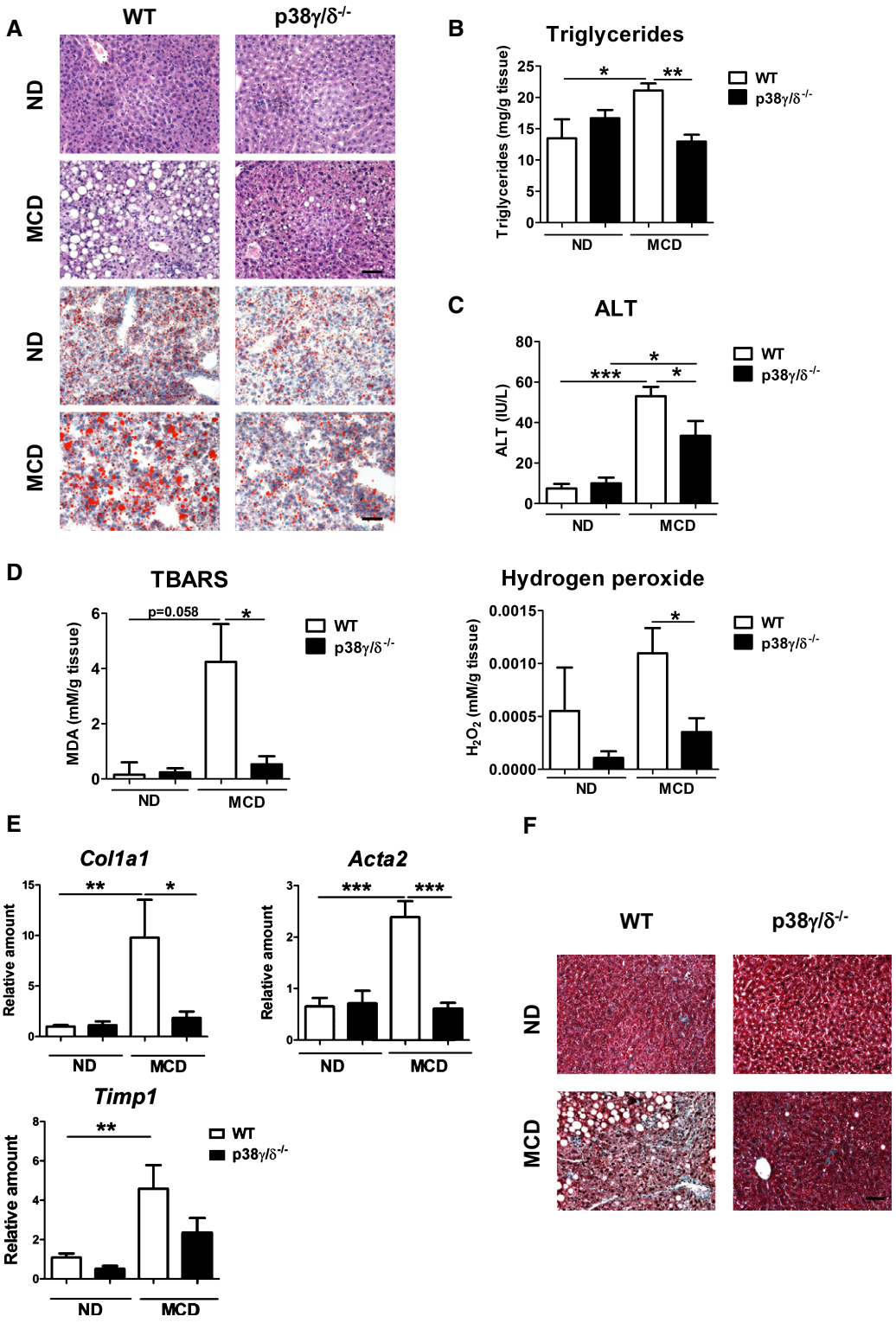

Figure 2. p38γ/δ$^{-/-}$ mice are protected against steatohepatitis and fibrosis.

A Representative H&E- and Oil Red-stained liver sections prepared from WT and p38γ/δ$^{-/-}$ mice fed a ND or the MCD diet for 3 weeks. Scale bar: 50 μm.

B, C Liver triglycerides (B) and plasma transaminase activity (ALT) (C) measured in WT and p38γ/δ$^{-/-}$ mice after 3 weeks of MCD diet.

D TBARS and hydrogen peroxide detected in liver samples from mice fasted overnight after the 3-week MCD diet.

E qRT–PCR analysis of *Col1a1*, *Acta2*, and *Timp1* mRNA expression. mRNA expression was normalized to the amount of *Gapdh* mRNA.

F Representative Masson's trichrome-stained liver sections prepared from WT and p38γ/δ$^{-/-}$ mice fed a ND or the MCD diet for 3 weeks. Scale bar: 50 μm.

Data information: Data are means ± SEM (n = 5–10). *P < 0.05; **P < 0.01; ***P < 0.001 (one-way ANOVA coupled to Bonferroni's post-tests).

levels of the myeloid cell marker *F4/80* and the cytokines *Tnfa* and *Il6* were significantly lower in p38γ/δ$^{-/-}$ mice than in WT mice (Appendix Fig S2B). However, analysis of M1 and M2 macrophage-differentiation markers revealed no differences in M1 (*Ifng*, *Il23)* and M2 markers (*Il10, Il13* or *Arg)* between WT and p38γ/δ$^{-/-}$ mice (Appendix Fig S2C).

Effect of myeloid cell expression of p38γ and p38δ on MCD-induced steatosis

To elucidate the role of myeloid-expressed p38γ/δ in the development of steatosis, we analyzed mice lacking p38γ/δ in myeloid cells. These mice have complete deletion of p38γ and p38δ in macrophages, and neutrophils infiltrated in liver and spleen while only partial deletion of p38δ was observed in dendritic cells (Appendix Fig S3A). Control mice expressing Cre recombinase (Lyzs-Cre mice) developed the typical hepatic steatosis in response to the MCD diet, with associated liver accumulation of triglycerides and hepatocyte necrosis indexed by serum ALT (Fig 3A–C). In contrast, the response of p38γ/δ$^{Lyzs\text{-}KO}$ mice to the MCD diet was milder for all three parameters (Fig 3A–C), demonstrating a protection similar to that seen in global p38γ/δ$^{-/-}$ mice. The p38γ/δ$^{Lyzs\text{-}KO}$ mice also had lower circulating levels of TNF-α and IL-6 than Lyzs-Cre mice after the MCD diet (Fig 3D), and gene expression analysis revealed significantly lower levels of the pro-inflammatory and myeloid cell markers *Il6, Gr1, Lyzs*, and *F4/80* (Fig 3E). In contrast, there were no between-genotype differences in the M1/M2 polarization of liver-infiltrated macrophages (Fig 3F).

Myeloid-specific p38γ and p38δ deficiencies do not affect diet-induced obesity, but protect against steatosis and diabetes

To confirm that the protection against liver steatosis in MCD-diet p38γ/δ$^{Lyzs\text{-}KO}$ mice was independent of the model used to induce the disease, we fed Lyzs-Cre and p38γ/δ$^{Lyzs\text{-}KO}$ mice with a high-fat diet (HFD). Weight gain was the same in p38γ/δ$^{Lyzs\text{-}KO}$ and Lyzs-Cre mice (Fig 4A), consistent with their similar lean and fat mass (Fig 4B). Liver mass was slightly lower in p38γ/δ$^{Lyzs\text{-}KO}$ mice (Fig 4C), while white adipose tissue mass was similar in both genotypes (Fig 4D). Histological analysis revealed less severe liver HFD-induced steatosis in the p38γ/δ$^{Lyzs\text{-}KO}$ mice (Fig 5A and B), correlating with lower circulating ALT levels (Fig 5C). We found higher energy expenditure in p38γ/δ$^{Lyzs\text{-}KO}$ animals with no differences in the respiratory exchange quotient [VCO_2]/[VO_2] between p38γ/δ$^{Lyzs\text{-}KO}$ and Lyzs-Cre mice (Fig 4E).

To study whether the protection against steatosis ameliorates HFD-induced diabetes, we performed a glucose tolerance test (GTT). HFD-fed p38γ/δ$^{Lyzs\text{-}KO}$ mice showed significantly higher glucose tolerance (Fig 5D) and lower fasting glucose (Fig 5E) than age-matched Lyzs-Cre controls on the same diet. These results indicate that the protection against steatosis in mice lacking p38γ/δ in myeloid cells also protects against HFD-induced diabetes.

A diet high in cholesterol, saturated fat, and fructose (HFF) has been found to recapitulate features of metabolic syndrome and NASH better than the traditional HFD (Charlton *et al*, 2011). Histological analysis of p38γ/δ$^{Lyzs\text{-}KO}$ and Lyzs-Cre mice fed a HFF diet revealed less severe liver steatosis in the p38γ/δ$^{Lyzs\text{-}KO}$ mice (Appendix Fig S3B and F), inflammation and fibrosis (Appendix Fig S3F), correlating with lower triglyceride accumulation and circulating ALT levels (Appendix Fig S3C and D). This protection against liver steatosis was associated with an improvement in fasting glucose (Appendix Fig S3E).

p38γ-floxed mice have below-normal expression of p38γ in muscle and fat (data not shown), raising the possibility that this defective expression might contribute to the protection against steatosis. To exclude this, we generated radiation chimeras by transplanting p38γ/δ$^{Lyzs\text{-}KO}$ or Lyzs-Cre bone marrow cells into lethally irradiated WT mice and fed a HFD or MCD diet. Efficient reconstitution of B6.SJL (CD45.1) mice with p38γ/δ$^{Lyzs\text{-}KO}$ or Lyzs-Cre bone marrow from C57BL/6J (CD45.2) mice was confirmed by staining peripheral blood leukocytes and liver-infiltrated leukocytes with antibodies to CD45.1/CD45.2 and analysis by flow cytometry (Fig 6A). Histological analysis showed milder steatosis (Fig 6B and C and Appendix Fig S4A), correlating with lower circulating ALT levels (Fig 6D and Appendix Fig S4B) after MCD or HFD in CX BM p38γ/δ$^{Lyzs\text{-}KO}$ than in the control CX BM Lyzs-Cre mice. Protection against HFD-induced steatosis associated with lower fasting glucose in CX BM p38γ/δ$^{Lyzs\text{-}KO}$ (Fig 6E). These results confirmed that this protection is a specific consequence of the loss of p38γ/δ in bone marrow-derived cells.

p38γ and p38δ control neutrophil infiltration during steatosis by regulating neutrophil adhesion

The protection of p38γ/δ myeloid KO mice against steatosis and liver inflammation, together with the low levels of myeloid cell markers in the livers of these animals suggested a possible effect on liver infiltration in animals fed a MCD diet or HFD. Characterization of liver-infiltrating leukocyte subsets in mice fed either diet revealed that the diet-induced increase in liver-infiltrating neutrophil counts (CD11b^{+}Gr-1^{high}) was significantly bigger in Lyzs-Cre mice than in p38γ/δ$^{Lyzs\text{-}KO}$ mice (Fig 7A), and similar results were observed in radiation chimeras restored by bone marrow from Lyzs-Cre mice versus p38γ/δ$^{Lyzs\text{-}KO}$ mice (Appendix Figs S4C and S5). This result correlated with lower levels of circulating neutrophils in p38γ/δ$^{Lyzs\text{-}KO}$ mice after both diets (Fig 7B and C).

Figure 3. p38γ/δ$^{Lyzs\text{-}KO}$ mice are protected against steatohepatitis induced by MCD diet.
Lyzs-Cre and p38γ/δ$^{Lyzs\text{-}KO}$ mice were fed a ND or a MCD diet for 3 weeks.

A Representative H&E- and Oil Red-stained liver sections. Scale bar: 50 μm.
B, C Liver triglycerides (B) and plasma ALT (C) at the end of the diet period.
D Measurement of plasma TNF-α and IL-6.
E qRT–PCR analysis of myeloid cell markers and cytokine mRNA expression from liver tissue; mRNA expression was normalized to the amount of *Gapdh* mRNA.
F qRT–PCR analysis of M1 and M2 polarization cell markers from liver-infiltrated macrophages. mRNA expression was normalized to the amount of *Gapdh* mRNA.

Data information: Data are means ± SEM (n = 5–10). *P < 0.05; **P < 0.01; ***P < 0.001 (one-way ANOVA coupled to Bonferroni's post-tests).

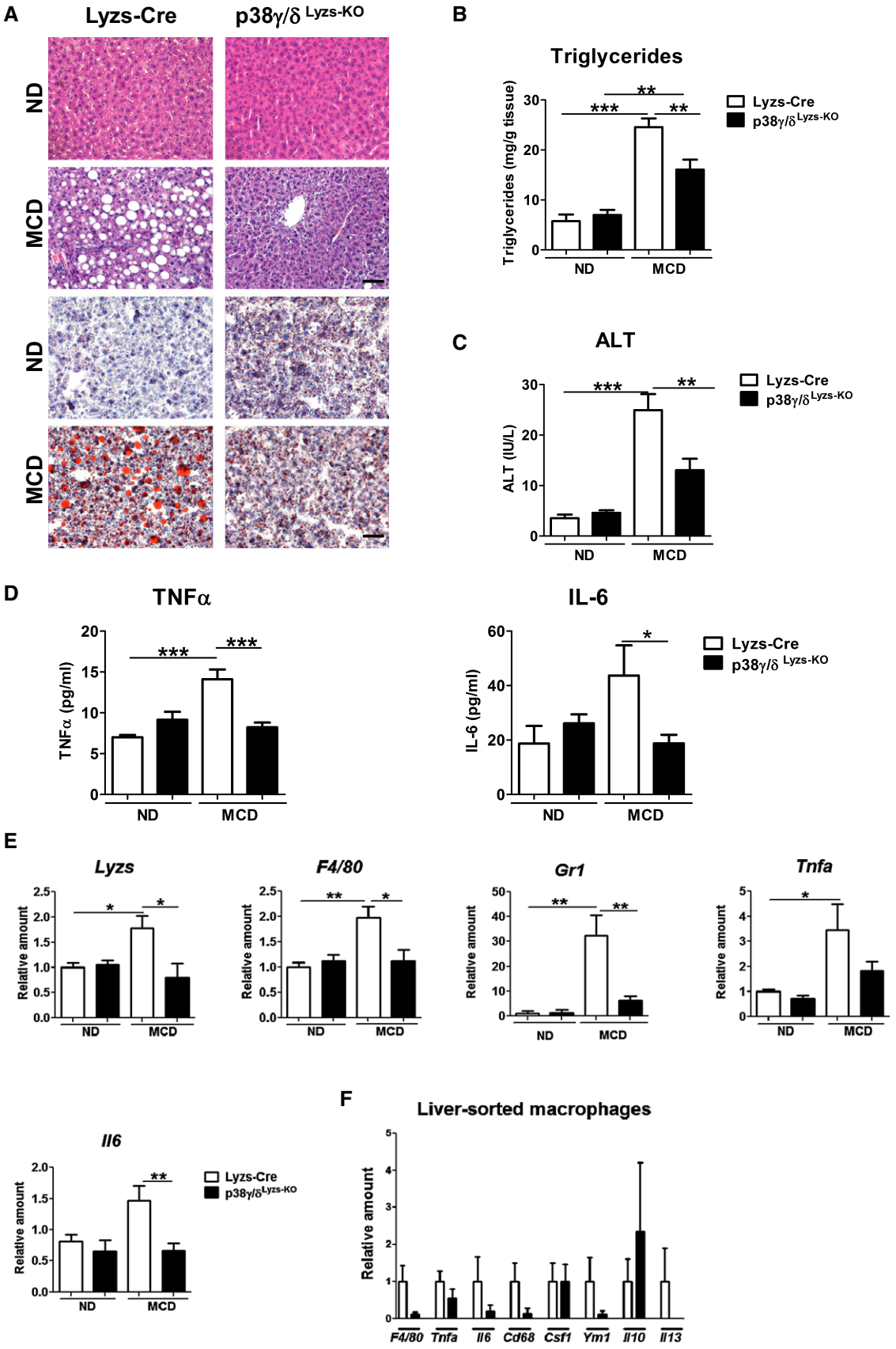
A
Lyzs-Cre
p38γ/δ Lyzs-KO
ND
MCD
ND
MCD
B
Triglycerides
Triglycerides (mg/g tissue)
Lyzs-Cre
p38γ/δ Lyzs-KO
ND
MCD
C
ALT
ALT (IU/L)
Lyzs-Cre
p38γ/δ Lyzs-KO
ND
MCD
D
TNFα
TNFα (pg/ml)
ND
MCD
IL-6
IL-6 (pg/ml)
Lyzs-Cre
p38γ/δ Lyzs-KO
ND
MCD
E
Lyzs
F4/80
Gr1
Tnfa
Relative amount
ND
MCD
Il6
Lyzs-Cre
p38γ/δ Lyzs-KO
F
Liver-sorted macrophages
Relative amount
F4/80
Tnfa
Il6
Cd68
Csf1
Ym1
Il10
Il13

Figure 3.

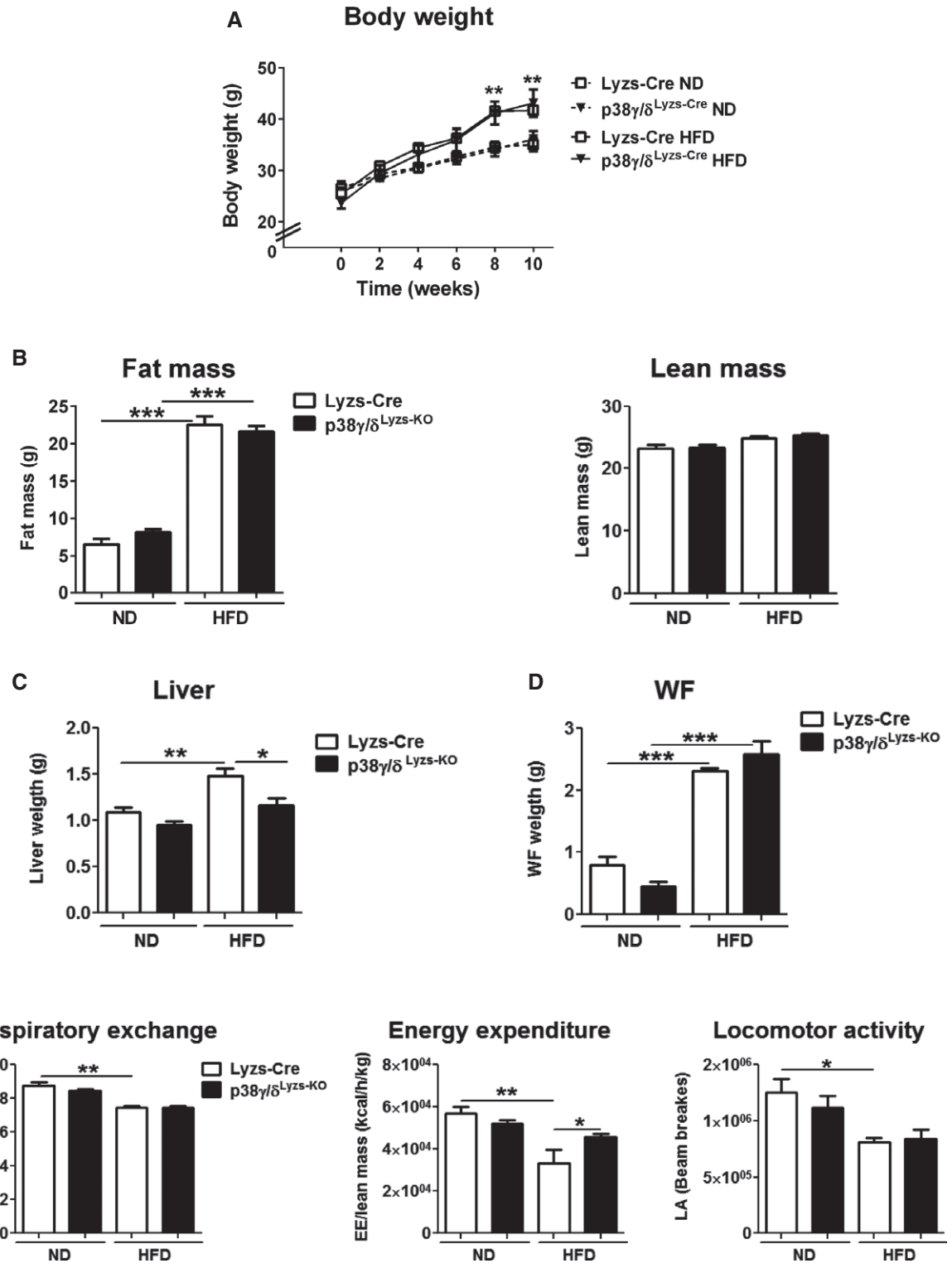

Figure 4. p38γ and p38δ deficiency in myeloid cells improves glucose metabolism in an obesity model.

Lyzs-Cre and p38γ/δ$^{Lyzs-KO}$ mice were fed a ND or a high-fat diet (HFD) for 10 weeks.

A Body weight measured at the indicated times during HFD treatment.

B Fat mass and lean mass determined by MRI at the end of the diet period.

C, D Liver mass and white fat (WF) mass.

E Respiratory exchange quotient, energy expenditure, and locomotor activity, detected in metabolic cages.

Data information: Data are means ± SEM (n = 5–10). *P < 0.05; **P < 0.01; ***P < 0.001 (one-way ANOVA coupled to Bonferroni's post-tests).

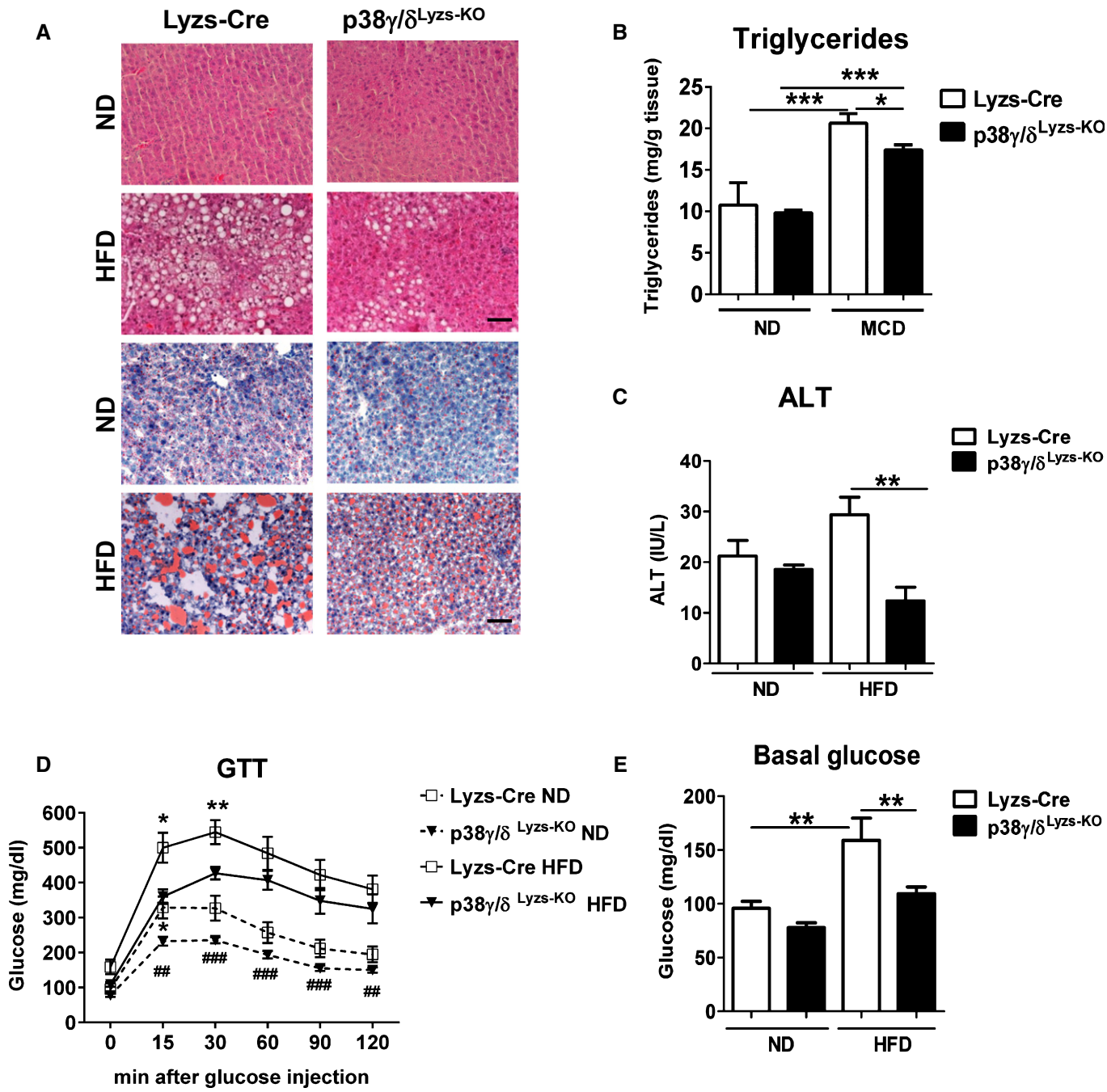

Figure 5. p38γ/δ$^{Lyzs-KO}$ mice are protected against steatohepatitis induced by HFD.

Lyzs-Cre and p38γ/δ$^{Lyzs-KO}$ mice were fed a ND or a HFD for 10 weeks.

A, B Representative H&E- and Oil Red-stained liver sections (scale bar: 50 μm) (A) and liver triglycerides (B).

C Plasma ALT at the end of the diet period.

D Glucose tolerance measured at the end of the diet period. Blood glucose concentration was measured in mice given an intraperitoneal glucose injection (1 g/kg) after overnight fasting.

E Basal blood glucose in overnight-fasted ND and HFD-fed Lyzs-Cre and p38γ/δ$^{Lyzs-KO}$ mice.

Data information: Data are means ± SEM (n = 5–10). *P < 0.05; **P < 0.01; ***P < 0.001 refers to p38γ/δ$^{Lyzs-KO}$ versus Lyzs-Cre; $^{\#\#}P$ < 0.01; $^{\#\#\#}P$ < 0.001 refers to ND versus HFD (one-way ANOVA coupled to Bonferroni's post-tests or Newman–Keuls post-test for liver triglycerides).

Neutrophils are the first immune cell type to respond to inflammation and can induce a chronic inflammatory state by promoting macrophage recruitment and interacting with antigen-presenting cells (Mantovani *et al*, 2011; Talukdar *et al*, 2012). Neutrophil levels by defensin 1–3 and neutrophils activation by nitrotyrosine staining, a measure of NO production, were elevated in the livers of obese

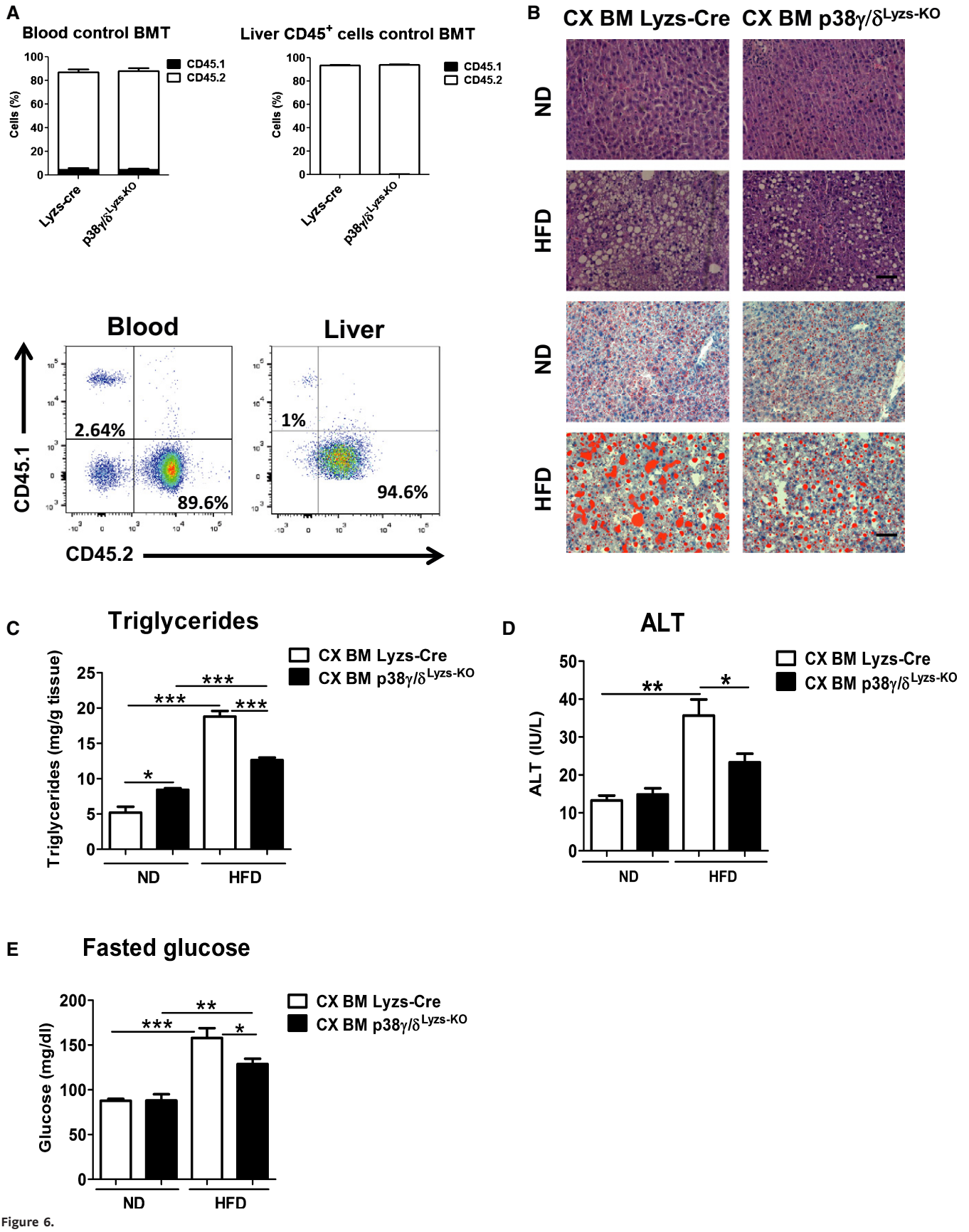

Figure 6.

Figure 6. p38γ/δ$^{Lyzs\text{-}KO}$ hematopoietic cells protect mice against HFD-induced steatosis.

Lethally irradiated WT mice were reconstituted with BM from Lyzs-Cre (Cx BM Lyzs-Cre) or p38γ/δ$^{Lyzs\text{-}KO}$ mice (Cx BM p38γ/δ$^{Lyzs\text{-}KO}$). Two months after the transplant, mice were fed the HFD for 10 weeks.

A Freshly prepared CD45.2 whole BM mononuclear cells (2×10^7) were transplanted into lethally irradiated B6.SJL (CD45.1) mice, and engraftment by CD45.2 cells (%) was analyzed by antibody staining and FACS of peripheral blood and liver CD45$^+$ cells. Charts show CD45.1 and CD45.2 expression in blood cells (left) and liver cells (right) isolated from transplanted mice (n = 3). Representative FACS dot plots of CD45.1 and CD45.2 expression are shown beneath the charts.

B Representative H&E- and Oil Red-stained liver sections. Scale bar: 50 μm.

C Liver triglyceride content.

D Plasma transaminase ALT activity.

E Fasted glucose, detected at the end of the diet period in overnight-fasted mice.

Data information: Data are means ± SEM (n = 5–10). *P < 0.05; **P < 0.01; ***P < 0.001 (one-way ANOVA coupled to Bonferroni's post-tests).

patients with NAFLD (Appendix Fig S6A and B). To test the possible role of neutrophil p38γ/δ expression in the etiology of inflammation-induced liver steatosis, we first compared the capacity of WT and p38γ/δ-neutrophils to migrate to steatotic liver. For this, we performed a competitive cell migration assay that allows direct and simultaneous comparison of the migration of multiple cell subsets in the same mouse. MCD-diet WT mice were i.v. injected with a 1:1 mix of DiO-labeled WT and DiD-labeled p38γ/δ$^{-/-}$ neutrophils (6×10^6 cells in total). WT neutrophils arrived at the steatotic liver 1 h after injection, but recruitment of p38γ/δ$^{-/-}$ neutrophils was markedly curtailed (Fig 7D and E). The more extensive recruitment of WT neutrophils appear to be not due to better survival since neutrophils from both genotypes showed the same survival ratio; however, we cannot rule out some role of p38γ/δ in neutrophil survival (Appendix Fig S7A).

Using intravital microscopy (IVM), we further quantified TNF-α-stimulated neutrophil migration in the microcirculation of the cremaster muscle of mice reconstituted with bone marrow (BM) from Lyzs-Cre or p38γ/δ$^{Lyzs\text{-}KO}$ mice (Movies EV1 and EV2). Numbers of rolling neutrophils were slightly higher in mice receiving p38γ/δ$^{Lyzs\text{-}KO}$ BM, accompanied by higher rolling velocity and contrasting with lower numbers of adherent neutrophils (Fig 7F). This higher rolling velocity is consistent with increased expression of L-selectin observed in neutrophils lacking p38γ/δ. Moreover, the defective adhesion might be explained by the lower expression in p38γ/δ$^{Lyzs\text{-}KO}$ neutrophils of CD11b, an integrin that regulates neutrophil adhesion and migration (Appendix Fig S7B). These results show that neutrophil adhesion and recruitment are compromised in the absence of p38γ/δ. Neutrophil rolling under flow conditions is mediated by L-selectin (Abbassi *et al*, 1993). To test the involvement L-selectin in the impaired rolling of p38γ/δ$^{Lyzs\text{-}KO}$ neutrophils, we assayed neutrophil migration under flow conditions on plates coated with the CD11b ligand ICAM-1 and the L-selectin ligand E-selectin. Our results indicated that p38γ/δ$^{Lyzs\text{-}KO}$ neutrophils presented a higher rolling velocity than Lyzs-Cre neutrophils (Appendix Fig S7C).

To investigate whether the altered migration capacity of p38γ/δ$^{Lyzs\text{-}KO}$ neutrophils is due to an autonomous effect or a defective production of chemokines, we performed a parabiosis experiment. Efficiency of parabiosis was evaluated by using congenic markers to distinguish blood cells in parabiotic pairs, in which one partner was CD45.1$^+$. Parabiotic exposure of p38γ/δ$^{Lyzs\text{-}KO}$ mice to the circulation of WT (CD45.1) mice, both fed the MCD diet, was enough to worsen the steatosis phenotype of p38γ/δ$^{Lyzs\text{-}KO}$ (Appendix Fig S8A). The exacerbated steatosis correlated with a higher proportion of CD45.1 (WT) neutrophils in p38γ/δ$^{Lyzs\text{-}KO}$ livers compared to the proportion observed in livers from Lyzs-Cre mice (Appendix Fig S8B). There were no differences in macrophage infiltration (Appendix Fig S8B), indicating that the wild-type circulation specifically increases liver neutrophil infiltration in p38γ/δ$^{Lyzs\text{-}KO}$ mice. Neutrophils thus appear to be crucial to the steatosis protection in p38γ/δ$^{Lyzs\text{-}KO}$ mice.

Neutrophil-specific p38δ deficiency protects against steatosis

The most abundant p38 isoform in neutrophils is p38δ (Ittner *et al*, 2012). To test the implication of neutrophil p38δ in liver steatosis, we crossed p38δ-floxed mice with Mrp8-Cre mice (Passegue *et al*, 2004) to generate mice lacking p38δ specifically in neutrophils (p38δ$^{Mrp8\text{-}KO}$ mice; Appendix Fig S9A). H&E and Oil Red staining of liver sections revealed that these mice were partially protected against MCD-induced steatosis (Appendix Fig S9B). Moreover, p38δ$^{Mrp8\text{-}KO}$ mice had below-normal levels of MCD-induced ALT (Appendix Fig S9C). This protection was associated with low

Figure 7. p38γ/δ$^{Lyzs\text{-}KO}$ neutrophils have deficient migration to the liver.

A Flow cytometry analysis of liver myeloid subsets (CD11b$^+$ Gr-1^{high}, CD11b$^+$ Gr-1^{intermediate}, CD11b$^+$ Gr-1$^-$) isolated from Lyzs-Cre and p38γ/δ$^{Lyzs\text{-}KO}$ mice fed a MCD for 3 weeks or HFD for 10 weeks. Representative dot plots are shown, and bar charts show the diet-induced increase in each population as a percentage of the total intrahepatic CD11b$^+$ leukocyte population. Myeloid infiltrating cells isolated from livers were sorted by FACS and stained with H&E. Representative cells are shown next to the appropriate myeloid subsets.

B, C Neutrophils and monocytes as a percentage of total circulating leukocytes, measured in total blood in animals fed the MCD diet for 3 weeks (B) or the HFD for 10 weeks (C).

D, E WT mice fed the MCD diet were i.v. injected with a 1:1 mix of DiO-labeled Lyzs-Cre neutrophils and DiD-labeled p38γ/δ$^{Lyzs\text{-}KO}$ neutrophils (6×10^6 cells in total; n = 10). One hour after injection, liver-infiltrating neutrophils were assessed by flow cytometry (D) and fluorescence micrography on liver sections (E).

F Intravital microscopy quantification of the rolling and adhesion frequencies and rolling velocities of neutrophils recruited to venules irrigating inflamed (TNF-α-injected) cremaster muscle.

Data information: Data are means ± SEM (n = 5–10). *P < 0.05; **P < 0.01; ***P < 0.001 (one-way ANOVA coupled to Bonferroni's post-tests).

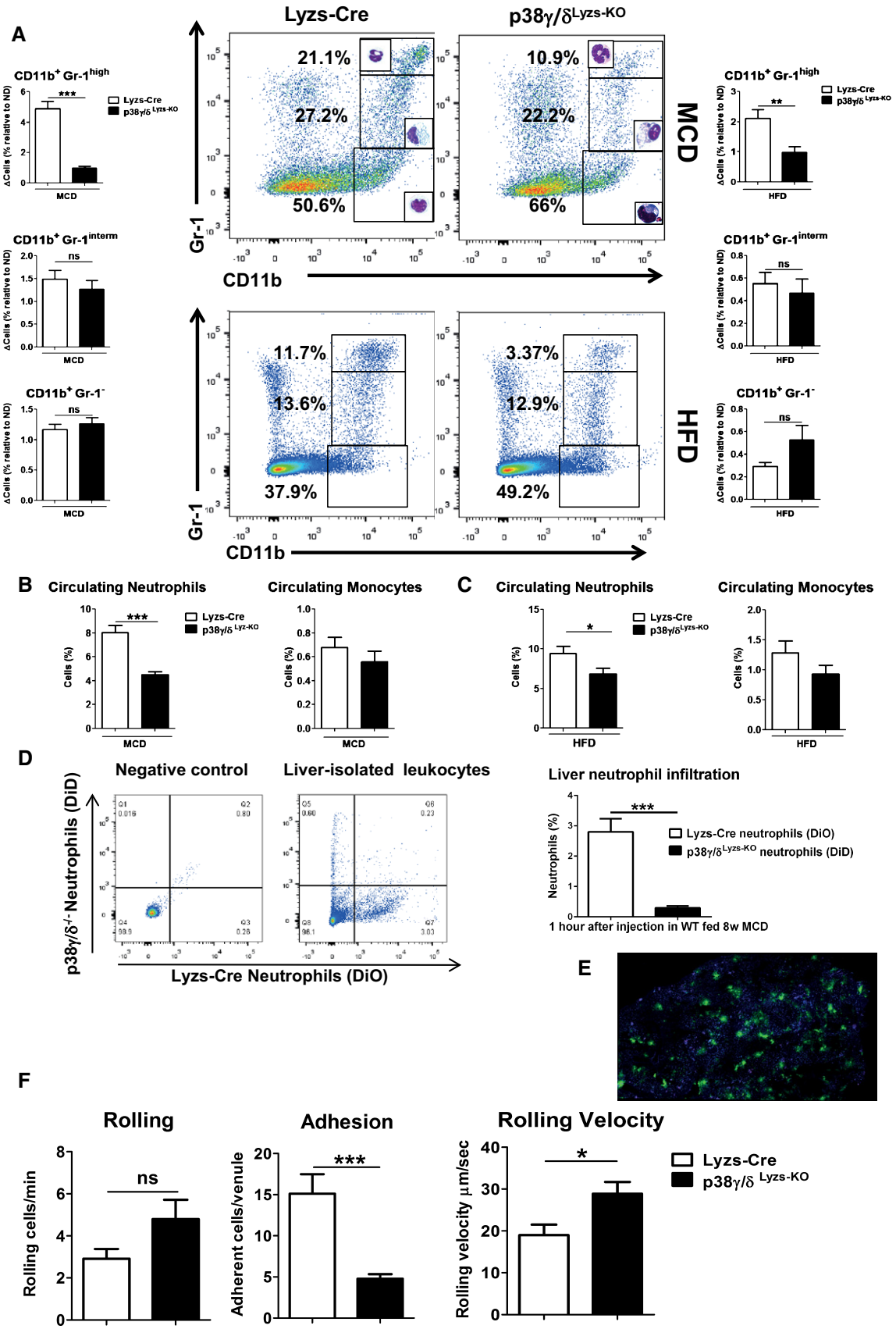

Figure 7.

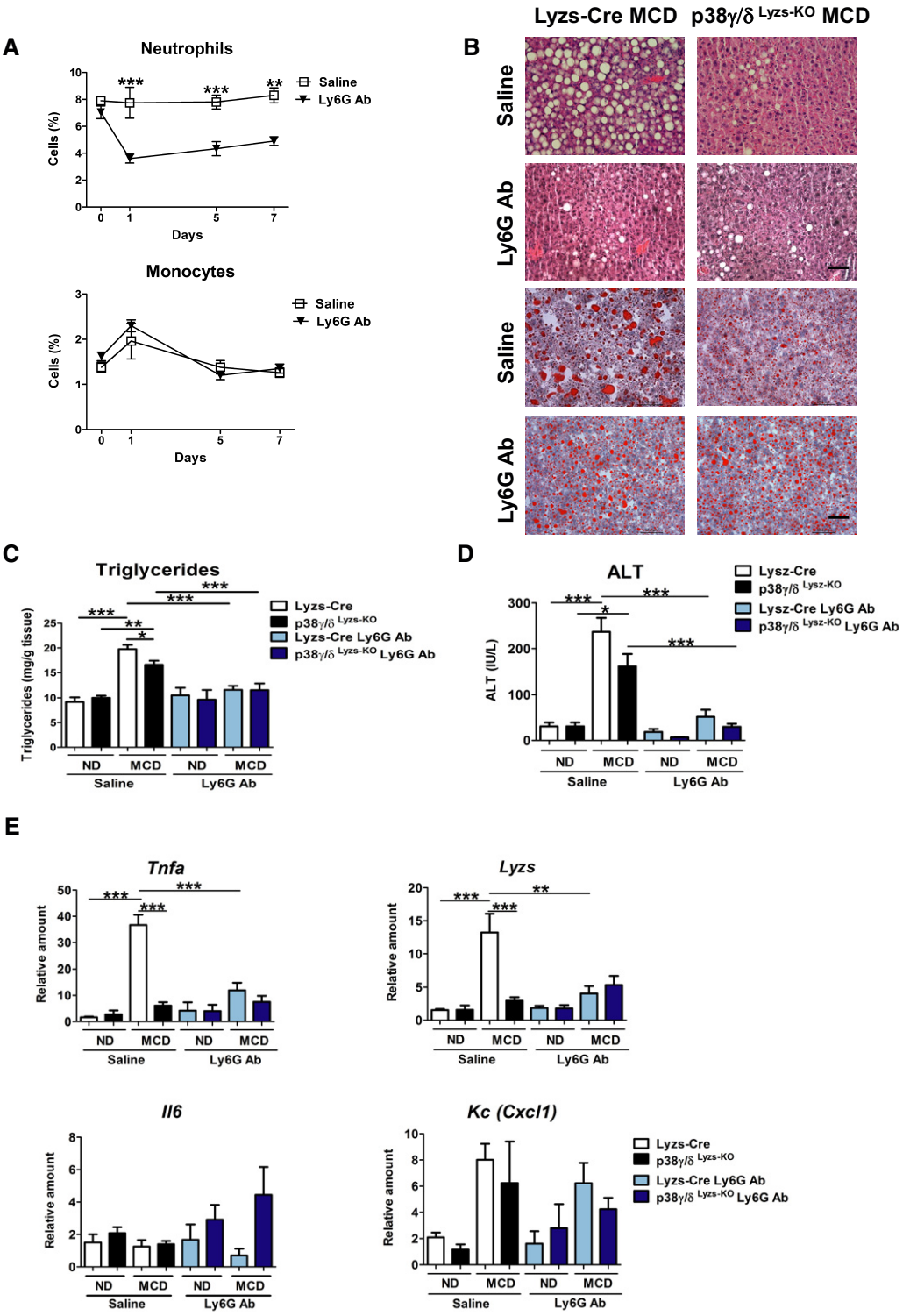

Figure 8. Neutrophil depletion protects against steatosis.

Osmotic minipumps containing saline or Ly6G antibody were implanted subcutaneously in Lyzs-Cre and p38γ/δ$^{Lyzs\text{-}KO}$ mice. These animals were fed a ND or MCD for 3 weeks.

A Neutrophils and monocytes as a percentage of circulating leukocytes, measured in total blood.

B Representative H&E- and Oil Red-stained liver sections after 3 weeks of treatment. Scale bar: 50 μm.

C, D Liver triglyceride (C) and plasma transaminase activity (ALT) (D) at the end of the diet period.

E Total RNA was extracted from livers, and chemokine and cytokine mRNA levels were determined by qRT–PCR. mRNA expression was normalized to the amount of *Gapdh* mRNA.

Data information: Data are means ± SEM (n = 5–10). *P < 0.05; **P < 0.01; ***P < 0.001 (one-way ANOVA coupled to Bonferroni's post-tests).

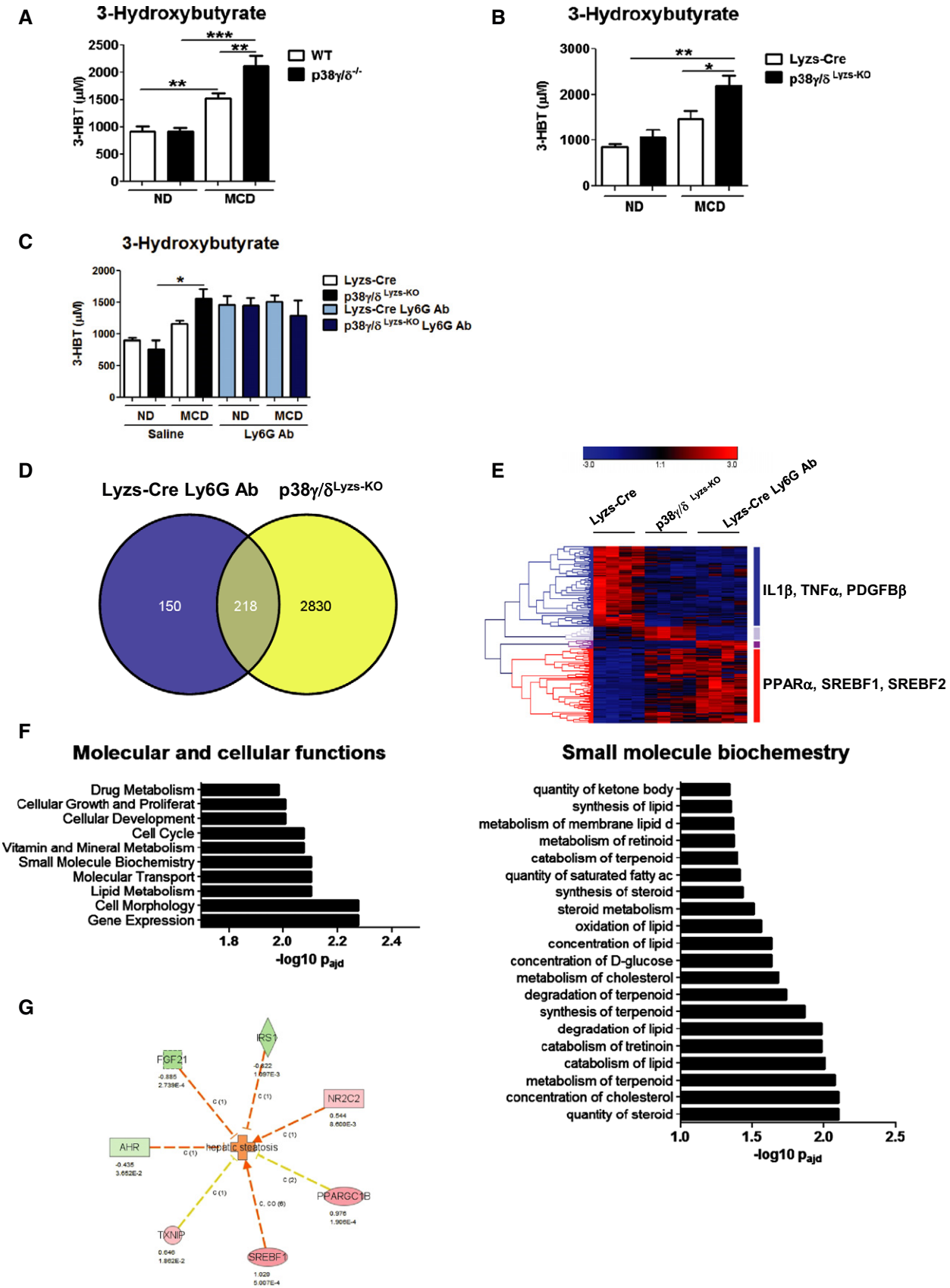

Figure 9.

neutrophil infiltration of the liver compared with MCD-diet-fed Mrp8-Cre mice (Appendix Fig S9D). These results indicate that the protection against steatosis is at least partially due to the expression of p38δ in neutrophils.

Neutrophil depletion protects against steatosis development

Early neutrophil accumulation triggers monocyte migration and inflammation (Savill *et al*, 1989), and diminished neutrophil accumulation can ameliorate NAFLD (Nathan, 2006). To clarify whether defective neutrophil migration contributes to the milder hepatic steatosis in MCD-diet p38γ/δ$^{Lyzs\text{-}KO}$ mice, we depleted neutrophils in MCD-diet Lyzs-Cre mice by administering anti-Ly6G antibody. Administration of this antibody (0.4 mg/kg per day i.v. for 7 days) reduced the levels of circulating neutrophils without affecting monocytes (Fig 8A), and treatment for 21 days significantly improved liver steatosis and reduced triglyceride accumulation to an extent similar to that observed in the MCD-diet p38γ/δ$^{Lyzs\text{-}KO}$ mice; in contrast, anti-Ly6G treatment of MCD-diet p38γ/δ$^{Lyzs\text{-}KO}$ mice did not appear to provide further benefit (Fig 8B and C). Anti-Ly6G antibody treatment of MCD-diet Lyzs-Cre animals also reduced liver necrosis assessed by serum ALT levels (Fig 8D). Moreover, while liver expression of *Il6* was not affected neutrophil depletion in Lyzs-Cre mice also significantly reduced liver expression of the pro-inflammatory markers *Tnfa* and *Lyzs* (Fig 8E).

Neutrophil depletion protects against steatosis by modulating lipid metabolism

We next measured the fatty-acid oxidation metabolite β-hydroxybutyrate, to investigate whether the improvement in hepatic steatosis in MCD-diet p38γ/δ$^{-/-}$, p38γ/δ$^{Lyzs\text{-}KO}$, and Ly6G-treated mice was linked to an increase in lipid oxidation. p38γ/δ$^{-/-}$, p38γ/δ$^{Lyzs\text{-}KO}$, and Ly6G-treated mice all had higher levels of serum β-hydroxybutyrate than similarly fed WT or Lyzs-Cre mice (Fig 9A–C), and this higher lipid oxidation correlated with the higher energy expenditure observed in p38γ/δ$^{Lyzs\text{-}KO}$ mice (Fig 4E).

To confirm an effect of impaired neutrophil infiltration on liver lipid metabolism, we examined the effect of MCD-diet on hepatic gene expression in Lyzs-Cre, p38γ/δ$^{Lyzs\text{-}KO}$, and anti-Ly6G-treated Lyzs-Cre mice by RNA-seq (Fig 9D–G). Differentially regulated genes that potentially contribute to the hepatic phenotype of the neutrophil-deficient mice were identified by comparing gene expression patterns with MCD-diet-fed Lyzs-Cre mice (Fig 9D–G). Most gene alterations observed in p38γ/δ$^{Lyzs\text{-}KO}$ mice were also detected in anti-Ly6G-treated Lyzs-Cre mice (Fig 9D). Gene ontology analysis of genes that changed in the same manner in both mice identified significant (adjusted $P < 0.001$) association of neutrophil deficiency with elevated oxidative lipid metabolism and decreased inflammation (Fig 9E), including genes regulated by PPAR-α (peroxisome proliferator-activated receptor-alpha) and by IL-2β and TNF-α (Fig 9E). Neutrophil deficiency thus causes increased lipid oxidation and decreased inflammation (Fig 9E–G).

Discussion

The alternative p38 MAPKs p38γ and p38δ regulate inflammatory processes through several mechanisms. Here, we demonstrate that expression of both kinases in myeloid cells is necessary for the development of liver steatosis and inflammation in animal models of NAFLD. Further, these kinases control neutrophil migration to the liver, and hepatic neutrophils contribute to liver steatosis by promoting liver inflammation and lipogenic metabolism. Deletion of p38γ/δ expression in the myeloid compartment curtails neutrophil recruitment to the liver, protecting animals against diet-induced steatosis and associated liver damage, and effect that is also partially mediated by the lack of p38δ in neutrophils. These findings indicate a major role of p38γ/δ in controlling neutrophil recruitment during inflammation and suggest that inhibition of neutrophil trafficking is a potential treatment route for steatosis.

The analysis of NAFLD mouse models clearly demonstrates that the protection in p38γ/δ$^{-/-}$ mice is attributable to the loss of p38γ/δ expression in hematopoietic cells. The bone marrow transfer experiments and conditional KO animal results confirm that p38γ and δ expressions by hematopoietic cells drive steatosis in both diet-induced steatosis models. Neutrophils were recently shown to be important mediators of alcoholic fatty liver disease (Bertola *et al*, 2013), and p38δ is known to control neutrophil inflammatory response in lung by regulating PKD1 activity (Ittner *et al*, 2012). Our analysis shows that loss of p38γ and p38δ in neutrophils might be responsible for the protection observed in the KO animals. Livers from mice lacking p38γ and p38δ had lower neutrophil infiltration, and neutrophils lacking these kinases could not be recruited to the liver in a competition assay, indicating a cell autonomous effect. The low adhesion and higher rolling velocity detected in neutrophils lacking p38γ and p38δ are broadly consistent with previous reports using p38δ$^{-/-}$ animals (Ittner *et al*, 2012). We also observed lower

Figure 9. Neutrophils control liver metabolic changes in steatosis development.

A–C Plasma levels of 3-hydroxybutyrate in WT and p38γ/δ$^{-/-}$ (A), Lyzs-Cre and p38γ/δ$^{Lyzs\text{-}KO}$ mice (B) and Lyzs-Cre Ly6G Ab treated after MCD diet (C) (n = 5–10).

D Overlap of gene expression changes between Lyzs-Cre mice treated with anti-Ly6G and p38γ/δ$^{Lyzs\text{-}KO}$ at the end of the MCD diet period n = 4 (each n is a mix of two different animals).

E Hierarchical clustering of the expression profiles of genes differentially expressed both between p38γ/δ$^{Lyzs\text{-}KO}$ and MCD-diet-fed Lyzs-Cre and between Lyzs-Cre treated with anti-Ly6G and MCD-diet-fed Lyzs-Cre mice. Genes up-regulated in both comparisons (red cluster) were mainly regulated by PPAR-α, SREBF1, and SREBF2, while the enriched upstream regulators of genes down-regulated in both conditions versus the control group (blue cluster) were IL-1β, TNF-α, and PDGFB-β.

F IPA (http://ingenuity.com) functional categories enriched in the set of genes differentially expressed between p38γ/δ$^{Lyzs\text{-}KO}$ and MCD-diet-fed Lyzs-Cre and between Lyzs-Cre treated with anti-Ly6G and MCD-diet-fed Lyzs-Cre mice (n = 4).

G Genes differentially expressed between p38γ/δ$^{Lyzs\text{-}KO}$ and MCD-diet-fed Lyzs-Cre and between Lyzs-Cre treated with anti-Ly6G and MCD-diet-fed Lyzs-Cre mice and involved in liver steatosis according to IPA.

Data information: Data are means ± SEM. *$P < 0.05$; **$P < 0.01$; ***$P < 0.001$ (one-way ANOVA coupled to Bonferroni's post-tests).

CD11b and higher L-selectin membrane expression, which could account for these defects in adhesion and rolling observed in the neutrophils lacking p38γ and p38δ. Moreover, lack of p38δ alone is insufficient to reduce neutrophil infiltration after the MCD diet and protect against liver steatosis. The ability of p38γ to compensate for the loss of p38δ is somewhat surprising given the low expression level of p38γ in neutrophils (Gonzalez-Teran *et al*, 2013; Han *et al*, 2013). A possible explanation is that $p38\delta^{-/-}$ neutrophils might increase the activation or expression of p38γ as a compensatory mechanism. It is also possible that p38γ in another myeloid cell type (e.g. resident macrophages) contributes to neutrophil migration by controlling cytokine and chemokine production. However, the results of competition migration assays in which resident macrophages are WT, and of the parabiosis experiment, argue against this possibility. Further experiments will be needed to determine the specific roles of p38γ and p38δ in different myeloid subsets and how these two isoforms can compensate each other. However, a role of neutrophils is clear because lack of p38δ only in neutrophils is enough to protect against steatosis.

On the other hand, the fact that neutrophil-specific deletion of p38δ has a more marked effect on phenotype than the whole-body p38δ KO might indicate that p38δ has an opposing role in another tissue and thereby modulates biological actions in a tissue-specific fashion. Opposing effects in different tissues have been shown for the stress kinase JNK: deletion of this kinase in the liver induces steatosis whereas deletion in fat is protective (Sabio *et al*, 2008, 2009).

Our data point out an important role of p38γ/δ in neutrophils. The same level of protection against diet-induced steatosis observed in $p38\gamma/\delta^{Lyzs\text{-}KO}$ mice was also achieved in mice depleted of neutrophils with anti-Ly6G antibody. Moreover, deletion of p38δ in neutrophils reduces hepatic neutrophils infiltration and partially protected against steatosis. These observations strongly suggest that neutrophil recruitment to the liver is essential for the initiation and progression of NAFLD and that neutrophil p38γ/δ expression contributes to the progression of this disease. The central role for neutrophils in NAFLD is consistent with their roles in ethanol-induced liver damage (Bertola *et al*, 2013) and macrophage recruitment to damaged tissue in obesity (Mansuy-Aubert *et al*, 2013) and with the description of neutrophil elastase as an important mediator of obesity-induced diabetes (Talukdar *et al*, 2012; Mansuy-Aubert *et al*, 2013). The importance of infiltrating neutrophils in liver inflammatory responses is also indicated by the underexpression of inflammatory genes in MCD-diet-fed $p38\gamma/\delta^{Lyzs\text{-}KO}$ and neutrophil-depleted mice and by the increased lipid oxidation and reduced lipogenesis in the neutrophil-depleted mice.

The data from mouse models correlate well with the overexpression p38δ and p38γ in livers of individuals with NAFLD, regardless of BMI, which could indicate the involvement of these kinases in the development of steatosis. This elevated p38δ expression could be due to increased neutrophil influx to these livers, as neutrophils are known to express high levels of p38δ (Ittner *et al*, 2012; Gonzalez-Teran *et al*, 2013). Accordingly, we also observed elevated neutrophil activity in the livers of obese patients with NAFLD. It would be interesting to characterize the cell-type contribution to p38δ and p38γ expression in human liver. However, we cannot rule out important roles for p38δ and p38γ expressed in other cell types involved in steatosis development.

In summary, our findings indicate that neutrophil infiltration triggers the development of NAFLD and that p38γ/δ regulate this process by controlling neutrophil infiltration. Therefore, inhibition of p38γ/δ might represent a novel therapeutic target for NAFLD in humans, with the potential to limit injury and possibly prevent progression to NASH and cirrhosis.

Materials and Methods

Study population and sample collection

The study population included a group of obese adult patients with body mass index (BMI) ≥ 35 kg/m^2 and a liver biopsy compatible with NAFLD. Participants were recruited from patients undergoing elective bariatric surgery at the University Hospital of Salamanca. As controls, we included individuals with BMI < 35 kg/m^2 who underwent laparoscopic cholecystectomy for gallstones. These individuals were divided into two groups according to the presence of NAFLD: (i) controls without NALFD ($n = 11$) if they had no laboratory or histopathological evidence of NAFLD or other liver diseases; (ii) controls with NAFLD ($n = 9$) if they had a liver biopsy compatible with NAFLD. Therefore, three groups of subjects were included in the study: obese patients (BMI ≥ 35 kg/m^2) with NAFLD, controls with BMI < 35 without liver disease, and controls with BMI < 35 kg/m^2 and with NAFLD. Baseline characteristics of these groups are listed in Appendix Table S1.

Participants were excluded if they had a history of alcohol use disorders or excessive alcohol consumption (> 30 g/day in men and > 20 g/day in women), chronic hepatitis C or B, or if laboratory and/or histopathological data showed causes of liver disease other than NAFLD. The study was approved by the Ethics Committee of the University Hospital of Salamanca and all subjects provided written informed consent to undergo liver biopsy under direct vision during surgery.

Data were collected on demographic information (age, sex, and ethnicity), anthropomorphic measurements (BMI), smoking and alcohol history, coexisting medical conditions, and medication use. Before surgery, fasting venous blood samples were collected for determination of complete cell blood count, total bilirubin, aspartate aminotransferase (AST), alanine aminotransferase (ALT), total cholesterol, high-density lipoprotein, low-density lipoprotein, triglycerides, creatinine, glucose, and albumin.

A portion of each liver biopsy was fixed in 10% formalin and stained with hematoxylin–eosin and Masson's trichrome for standard histopathological analysis. The remaining portion was stored at −80°C for later protein was extraction. The presence of NAFLD was diagnosed using standard criteria, and severity of the disease was established using the NAFLD activity score (NAS) described by Kleiner (Kleiner *et al*, 2005).

Mice

Mice deficient for p38γ (B6.129-Mapk12tm1) and p38δ (B6.129-Mapk13tm1) were crossed with B6.129P2-Lyz2tm1(cre)Ifo/J mice or with B6.Cg-Tg(S100A8-cre,-EGFP)1Ilw/J mice backcrossed for 10 generations to the C57BL/6J background (Jackson Laboratory). Genotype was confirmed by PCR analysis of genomic DNA.

Radiation chimeras were generated by exposing recipient mice to 2 doses of ionizing radiation (625 Gy) and reconstituting them with 2×10^7 donor BM cells by injection into the tail vein. Proper reconstitution was checked in B6.SJL (CD45.1) control mice transplanted with CD45.2 BM mononuclear cells by immunostaining and FACS analysis of peripheral blood and liver $CD45^+$ cells. Mice were fed a standard chow diet or a methionine–choline-deficient (MCD) diet for 3 weeks (Research Diets Inc). Alternatively, mice were fed a high-fat diet (HFD) or a high-fat and high-fructose (HFF) diet (Research Diets Inc) for 10 weeks. For neutrophil depletion, mice were treated with anti-Ly6G antibody (0.4 mg/kg per day, 21 days) via subcutaneously implanted mini-osmotic pumps (Alzet); saline was administered as a control. All animal procedures conformed to EU Directive 86/609/EEC and Recommendation 2007/526/EC regarding the protection of animals used for experimental and other scientific purposes, enacted under Spanish law 1201/2005.

Hepatic peroxidation

Liver extracts were prepared by sonication (15 cycles) in cytoplasmic lysis buffer [25 mM Tris–HCl (pH 7.5), 10 mM NaCl, 1 mM EDTA, 100 mM $MgCl_2$, 1% NP-40, 0.1 mM phenylmethylsulfonyl fluoride, and 10 μg/ml aprotinin and leupeptin]. Malondialdehyde and hydrogen peroxide were assayed with the TBARS Assay kit (Cayman) and the Amplex Red Hydrogen Peroxide/Peroxidase Assay Kit (Invitrogen).

Glucose tolerance test

Glucose tolerance test was performed as described (Mora *et al*, 2005).

Isolation of liver-infiltrating mononuclear leukocytes

Mouse livers were collected, and a single-cell suspension was obtained and passed through a 70-μm strainer. Leukocytes were collected from the interphase of centrifuged Ficoll gradients.

Flow cytometry

Isolated liver-infiltrating leukocytes were counted with a CASY Cell Counter (57) and then labeled by surface staining (Streptavidin-PERCP/biotin-conjugated anti-CD11b and APC-conjugated anti-Gr-1; Invitrogen). Flow cytometry was performed with a FACScan cytofluorometer (FACS Canto BD), and data were collected and analyzed with FlowJo software.

Intravital microscopy

Intravital microscopy of the cremaster muscle after TNF-α injection (0.5 μg, intrascrotal injection) was performed as reported (Sreeramkumar *et al*, 2013) using an Axio Examiner Z.1 workstation (Zeiss, Germany). Fluorescently conjugated anti-Ly6G (1 mg/mouse) was injected immediately before acquisition to specifically identify neutrophils. Recorded videos were analyzed using Slidebook software (Intelligent Imaging Innovations). At least 30 venules were analyzed from 3 mice per group.

Competitive cell migration assay

Lyzs-Cre and $p38\gamma/\delta^{Lyzs\text{-}KO}$ neutrophils were isolated from bone marrow by labeling with biotin-conjugated anti-Ly6C/G antibody (BD Pharmigen) and magnetic streptavidin microbeads (Miltenyi Biotec) and then separating them on MACS MS columns (Miltenyi Biotec). Isolated Lyzs-Cre neutrophils were stained with DiO and $p38\gamma/\delta^{Lyzs\text{-}KO}$ neutrophils were stained with DiD (Vybrant Cell-Labeling Solution, Molecular Probes). Cell viability was checked by DAPI staining followed by FACS. The labeled cells were then mixed at a 1:1 ratio and injected (6×10^6 cells) into MCD-diet WT mice. After 1 h, liver-infiltrating mononuclear leukocytes were isolated and directly detected by FACS. Fluorescent neutrophils were also detected by confocal microscopy in OCT-cryopreserved liver sections.

Statistical analysis

Differences between experimental groups were examined for statistical significance by two-tailed Student's *t*-test or one-way ANOVA coupled to Bonferroni's and Newman–Keuls post-test. Characteristics of patients and controls were compared by means of Mann–Whitney *U*-test for quantitative variables and χ^2 or Fisher's tests for qualitative variables.

For more Materials and Methods, see the Appendix.

Expanded View for this article is available online.

Acknowledgements

We thank S. Bartlett for English editing, L. Manzanedo, A. Mateos, and O. Rozo for help with sample and data collection, and A. Molina for histological analysis. We are grateful to R.J. Davis for critical reading of the manuscript, R. González-Sarmiento for help with clinical study design. We thank the staff at the CNIC Genomics, Cellomics, and Bioinformatics units for technical support and help with data analysis. G.S. is an investigator of the Ramón y Cajal Program. B.G.T. is a fellow of FPI Severo Ochoa CNIC Program (SVP-2013-067639). I.G.N. is supported by a CNIC IPP FP7 Marie Curie Programme (PCOFUND-2012-600396). M.A.V. is a recipient of a Madrid Regional Government Fellowship. This work was funded by the following grants to G.S.: ERC 260464, EFSD 2030, MICINN SAF2010-19347, and Comunidad de Madrid S2010/BMD-2326; to M.M.: ISCIII and FEDER, PI10/01692, and I3SNS-INT12/049; to L.H.C.: Junta de Castilla y León GRS 681/A/11; to A.H.: SAF 2012-31142; to R.N.: MICINN BFU2012-35255, Xunta de Galicia EM 2012/039 and 2012-CP069; and to A.C.: MICINN SAF2010-19734. The CNIC is supported by the Ministerio de Economía y Competitividad and the Pro-CNIC Foundation.

Author contributions

BG-T, NM, IGN, and GS designed the study; BG-T, NM, IGN, MAV, VS, AM, GC, MLS, EB, LL-V, ER, VB, and GS performed experimental analysis; metabolic cages were performed by RN and SP-S; intravital microscopy was performed by VS and AH; *in vitro* neutrophil migration was performed by MLS and FS-M; MM designed and coordinated human study; MM, LH-C, JLT, and LO recruited subjects and were responsible for sample and data collection; AC provided reagents and BG-T, NM, IGN, and GS wrote the manuscript. All authors contributed to the revision of the manuscript and approved the final version.

Conflict of interest

The authors declare that they have no conflict of interest.

References

Abbassi O, Kishimoto TK, McIntire LV, Anderson DC, Smith CW (1993) E-selectin supports neutrophil rolling *in vitro* under conditions of flow. *J Clin Invest* 92: 2719 – 2730

Adams RH, Porras A, Alonso G, Jones M, Vintersten K, Panelli S, Valladares A, Perez L, Klein R, Nebreda AR (2000) Essential role of p38alpha MAP kinase in placental but not embryonic cardiovascular development. *Mol Cell* 6: 109 – 116

Allen M, Svensson L, Roach M, Hambor J, McNeish J, Gabel CA (2000) Deficiency of the stress kinase p38alpha results in embryonic lethality: characterization of the kinase dependence of stress responses of enzyme-deficient embryonic stem cells. *J Exp Med* 191: 859 – 870

Anstee QM, Goldin RD (2006) Mouse models in non-alcoholic fatty liver disease and steatohepatitis research. *Int J Exp Pathol* 87: 1 – 16

Beardmore VA, Hinton HJ, Eftychi C, Apostolaki M, Armaka M, Darragh J, McIlrath J, Carr JM, Armit LJ, Clacher C, Malone L, Kollias G, Arthur JS (2005) Generation and characterization of p38beta (MAPK11) gene-targeted mice. *Mol Cell Biol* 25: 10454 – 10464

Bertola A, Park O, Gao B (2013) Chronic plus binge ethanol feeding synergistically induces neutrophil infiltration and liver injury in mice: a critical role for E-selectin. *Hepatology* 58: 1814 – 1823

Charlton M, Krishnan A, Viker K, Sanderson S, Cazanave S, McConico A, Masuoko H, Gores G (2011) Fast food diet mouse: novel small animal model of NASH with ballooning, progressive fibrosis, and high physiological fidelity to the human condition. *Am J Physiol Gastrointest Liver Physiol* 301: G825 – G834

Criado G, Risco A, Alsina-Beauchamp D, Perez-Lorenzo MJ, Escos A, Cuenda A (2014) Alternative p38 MAPKs are essential for collagen-induced arthritis. *Arthritis Rheumatol* 66: 1208 – 1217

Fabbrini E, Sullivan S, Klein S (2010) Obesity and nonalcoholic fatty liver disease: biochemical, metabolic, and clinical implications. *Hepatology* 51: 679 – 689

Farrell GC, Larter CZ (2006) Nonalcoholic fatty liver disease: from steatosis to cirrhosis. *Hepatology* 43: S99 – S112

Gonzalez-Teran B, Cortes JR, Manieri E, Matesanz N, Verdugo A, Rodriguez ME, Gonzalez-Rodriguez A, Valverde A, Martin P, Davis RJ, Sabio G (2013) Eukaryotic elongation factor 2 controls TNF-alpha translation in LPS-induced hepatitis. *J Clin Invest* 123: 164 – 178

Han MS, Jung DY, Morel C, Lakhani SA, Kim JK, Flavell RA, Davis RJ (2013) JNK expression by macrophages promotes obesity-induced insulin resistance and inflammation. *Science* 339: 218 – 222

Ittner A, Block H, Reichel CA, Varjosalo M, Gehart H, Sumara G, Gstaiger M, Krombach F, Zarbock A, Ricci R (2012) Regulation of PTEN activity by p38delta-PKD1 signaling in neutrophils confers inflammatory responses in the lung. *J Exp Med* 209: 2229 – 2246

Kleiner DE, Brunt EM, Van Natta M, Behling C, Contos MJ, Cummings OW, Ferrell LD, Liu YC, Torbenson MS, Unalp-Arida A, Yeh M, McCullough AJ, Sanyal AJ (2005) Design and validation of a histological scoring system for nonalcoholic fatty liver disease. *Hepatology* 41: 1313 – 1321

Mansuy-Aubert V, Zhou QL, Xie X, Gong Z, Huang JY, Khan AR, Aubert G, Candelaria K, Thomas S, Shin DJ, Booth S, Baig SM, Bilal A, Hwang D, Zhang H, Lovell-Badge R, Smith SR, Awan FR, Jiang ZY (2013) Imbalance between neutrophil elastase and its inhibitor alpha1-antitrypsin in obesity alters insulin sensitivity, inflammation, and energy expenditure. *Cell Metab* 17: 534 – 548

Mantovani A, Cassatella MA, Costantini C, Jaillon S (2011) Neutrophils in the activation and regulation of innate and adaptive immunity. *Nat Rev Immunol* 11: 519 – 531

Marchesini G, Bugianesi E, Forlani G, Cerrelli F, Lenzi M, Manini R, Natale S, Vanni E, Villanova N, Melchionda N, Rizzetto M (2003) Nonalcoholic fatty liver, steatohepatitis, and the metabolic syndrome. *Hepatology* 37: 917 – 923

Mora A, Lipina C, Tronche F, Sutherland C, Alessi DR (2005) Deficiency of PDK1 in liver results in glucose intolerance, impairment of insulin-regulated gene expression and liver failure. *Biochem J* 385: 639 – 648

Nathan C (2006) Neutrophils and immunity: challenges and opportunities. *Nat Rev Immunol* 6: 173 – 182

Passegue E, Wagner EF, Weissman IL (2004) JunB deficiency leads to a myeloproliferative disorder arising from hematopoietic stem cells. *Cell* 119: 431 – 443

Risco A, del Fresno C, Mambol A, Alsina-Beauchamp D, MacKenzie KF, Yang HT, Barber DF, Morcelle C, Arthur JS, Ley SC, Ardavin C, Cuenda A (2012) p38gamma and p38delta kinases regulate the Toll-like receptor 4 (TLR4)-induced cytokine production by controlling ERK1/2 protein kinase pathway activation. *Proc Natl Acad Sci USA* 109: 11200 – 11205

Sabio G, Arthur JS, Kuma Y, Peggie M, Carr J, Murray-Tait V, Centeno F, Goedert M, Morrice NA, Cuenda A (2005) p38gamma regulates the localisation of SAP97 in the cytoskeleton by modulating its interaction with GKAP. *EMBO J* 24: 1134 – 1145

Sabio G, Das M, Mora A, Zhang Z, Jun JY, Ko HJ, Barrett T, Kim JK, Davis RJ (2008) A stress signaling pathway in adipose tissue regulates hepatic insulin resistance. *Science* 322: 1539 – 1543

Sabio G, Cavanagh-Kyros J, Ko HJ, Jung DY, Gray S, Jun JY, Barrett T, Mora A, Kim JK, Davis RJ (2009) Prevention of steatosis by hepatic JNK1. *Cell Metab* 10: 491 – 498

Sabio G, Davis RJ (2010) cJun NH2-terminal kinase 1 (JNK1): roles in metabolic regulation of insulin resistance. *Trends Biochem Sci* 35: 490 – 496

Sabio G, Kennedy NJ, Cavanagh-Kyros J, Jung DY, Ko HJ, Ong H, Barrett T, Kim JK, Davis RJ (2010) Role of muscle c-Jun NH2-terminal kinase 1 in obesity-induced insulin resistance. *Mol Cell Biol* 30: 106 – 115

Sabio G, Davis RJ (2014) TNF and MAP kinase signalling pathways. *Semin Immunol* 26: 237 – 245

Savill JS, Wyllie AH, Henson JE, Walport MJ, Henson PM, Haslett C (1989) Macrophage phagocytosis of aging neutrophils in inflammation. Programmed cell death in the neutrophil leads to its recognition by macrophages. *J Clin Invest* 83: 865 – 875

Sreeramkumar V, Leiva M, Stadtmann A, Pitaval C, Ortega-Rodriguez I, Wild MK, Lee B, Zarbock A, Hidalgo A (2013) Coordinated and unique functions of the E-selectin ligand ESL-1 during inflammatory and hematopoietic recruitment in mice. *Blood* 122: 3993 – 4001

Talukdar S, da Oh Y, Bandyopadhyay G, Li D, Xu J, McNelis J, Lu M, Li P, Yan Q, Zhu Y, Ofrecio J, Lin M, Brenner MB, Olefsky JM (2012) Neutrophils mediate insulin resistance in mice fed a high-fat diet through secreted elastase. *Nat Med* 18: 1407 – 1412

Tamura K, Sudo T, Senftleben U, Dadak AM, Johnson R, Karin M (2000) Requirement for p38alpha in erythropoietin expression: a role for stress kinases in erythropoiesis. *Cell* 102: 221 – 231

Tiniakos DG, Vos MB, Brunt EM (2010) Nonalcoholic fatty liver disease: pathology and pathogenesis. *Annu Rev Pathol* 5: 145 – 171

Vernon G, Baranova A, Younossi ZM (2011) Systematic review: the epidemiology and natural history of non-alcoholic fatty liver disease and non-alcoholic steatohepatitis in adults. *Aliment Pharmacol Ther* 34: 274 – 285

